Ultra-wideband Feed Systems for the EVN and SKA - Evaluated for VGOS

Jonas Flygare, Miroslav Pantaleev, John Conway, Michael Lindqvist, Leif Helldner, Magnus Dahlgren, Rüdiger Haas, Peter Forkman

Abstract The design of the Square Kilometer Array (SKA) project for radio astronomy is now materializing at a rapid speed; the EU Horizon 2020 RadioNet project BRoad-bAND (BRAND) has the ambition of delivering a decade bandwidth receiver for EVN. The ultra-wideband quad-ridge flared horn (QRFH) feed systems developed for these projects show good performance within the geodetic VLBI Global Observing System (VGOS) frame due to the overlapping frequency bands and reflector geometries. We estimate, through simulation, the system equivalent flux density (SEFD) of the two feed systems in the VGOS reflector and compare it to the existing system installed on one of the 13.2-m diameter reflectors of the Onsala twin telescopes (OTT). The two frequency bands analyzed cover $1.5-15.5$ GHz and $4.6-24$ GHz. Both systems show an SEFD better than 1,000 Jy over large parts of the respective frequency band — comparable to the $3-18$ GHz feed systems. For the SKA QRFH over $4.6-24$ GHz, the water vapor absorption line at 22 GHz is within the operational band; therefore we study the application of water-vapor radiometry in line-of-sight of the telescope.

Keywords VGOS, Water-vapor radiometry, EVN, SKA, QRFH

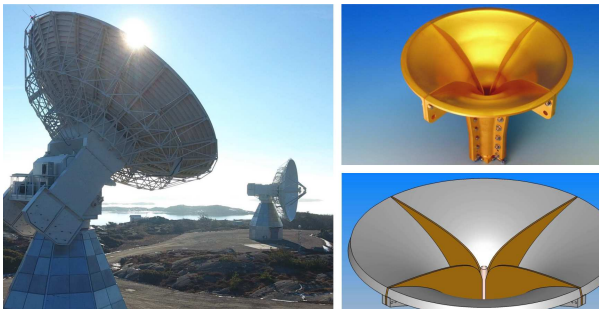

Fig. 1 (Left) Onsala Twin Telescopes, part of the VGOS network; (top right) SKA Band B QRFH: $4.6-24$ GHz; (bottom right) BRAND EVN QRFH: $1.5-15.5$ GHz.

1 Introduction

The ultra-wideband (UWB) Band B [2] feed was designed for $4.6-24$ GHz in the Square Kilometre Array (SKA) project as an option to extend the high-frequency limit beyond 13.8 GHz. UWB receivers enable large continuous bandwidth but also enable lower cost, less maintenance, and less complexity for a large telescope array compared to multiple narrowband receivers. The EU Horizon 2020 RadioNet project BRoad-bAND (BRAND) [3] for EVN has the ambition of offering a full decade receiver system that can replace multiple systems over L-, S-, C-, X-, and Ku-band with one receiver. Wideband feed systems are already installed and operational on the Onsala twin telescopes (OTT) within the VGOS network [1]. In Figure 1 (right) we present the two UWB quad-ridge flared horn (QRFH) feeds developed for these projects.

Onsala Space Observatory: Department of Space, Earth and Environment, Chalmers University of Technology

Due to the relatively large half-subtended angles these feeds were designed for, it is interesting to compare the system performance. We use the VGOS axial-symmetric ring-focus reflector in this comparison due to its relevance for the IVS community. The SKA QRFH excludes the generally RFI-polluted $2-4$ GHz band, due to the low-frequency cut-off property of the waveguide-based QRFH. An interesting application of the high-frequency limit of 24 GHz is the possibility of doing line-of-sight water-vapor radiometry on the telescope during observation. We compare this approach with dedicated water-vapor radiometers based on simulations. This offers an interesting upgrade of future frequency bands for VGOS.

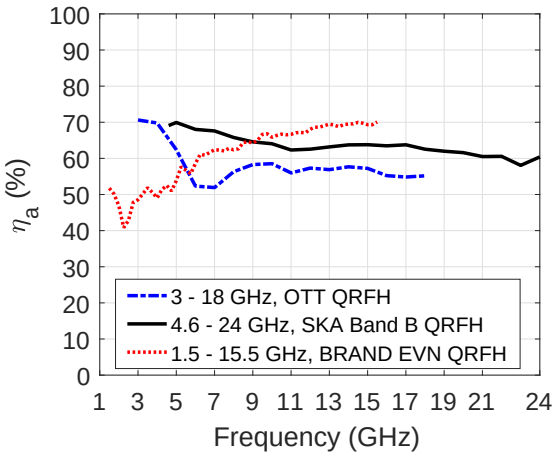

Fig. 2 Simulated aperture efficiency, η_a, over frequency for the three receiver systems in the OTT reflector.

2 System SEFD Performance

In Figures 2 through 4, we present the simulated system performance in the 13.2-m OTT reflector for the introduced receiver systems. We compare the performance to the current $3-18$ GHz QRFH system for OTT [1]. The OTT QRFH and SKA Band B QRFH results are based on measured beam patterns and receiver noise temperature determined through Y-factor tests with state of the art UWB low noise amplifiers (LNA). For the calculation of antenna noise temperature, T_A, a system simulator using physical optics (PO) and physical theory of diffraction (PTD) was used [4]. All three receiver setups show a system equivalent flux density (SEFD) better than 1,000 Jy over large parts of their respective frequency band for zenith ($\theta = 90^\circ$) in Figure 3. The elevation (θ) dependence of T_A is clearly seen in Figure 4, which degrades the SEFD closer to the horizon, specifically around the water-line at 22 GHz.

3 Water-Vapor Radiometry in Telescope Line-of-sight with High-frequency QRFH

Water-vapor radiometry (WVR) in line-of-sight (LOS) of the telescope, as previously investigated in [5], is an interesting application of high-frequency wide-band feed. We present a theoretical study estimating the zenith integrated cloud water (ICW) and zenith integrated water vapor (IWV) using the sky brightness temperatures at two frequencies in the $15-35$ GHz range. A similar study has previously been performed [6].

Vertical profiles of pressure, temperature, humidity, and cloud water are taken from the ERA-Interim reanalysis [7]. Data for two years (four times a day) at a grid point close to the Onsala Space Observatory have been used in the investigation. ARTS (Atmospheric Radiative Transfer System; [8]; [9]) was used to calculate the sky brightness temperatures from the ERA-Interim vertical profiles. ARTS is a general forward model for observations of thermal emission, often used for microwave applications. In the ARTS setup, [10] was used for the absorption of water-vapor and oxygen, [11] for the absorption of nitrogen, [12] for the air refractive index, and [13] for the absorption of liquid cloud water. In the $15-35$ GHz frequency range, scattering can be omitted as long as the droplets are smaller than about 0.5 mm. The simulations are therefore valid during clear or cloudy conditions but not during rainy weather. No mapping functions are needed because the ray tracing calculations include the Earth's curvature. The ERA-Interim data was used to derive IWV and ICW, and ARTS was used to simulate the sky brightness temperatures at certain elevations assuming a narrow beam. Figure 5 (top) shows the simulated sky brightness temperatures, T_b, at elevation $\theta = 30^\circ$ (two air-masses) for the two-year ERA-Interim data set. The peak around $20-25$ GHz is due to the absorption line of water-vapor at 22 GHz, while the general upward

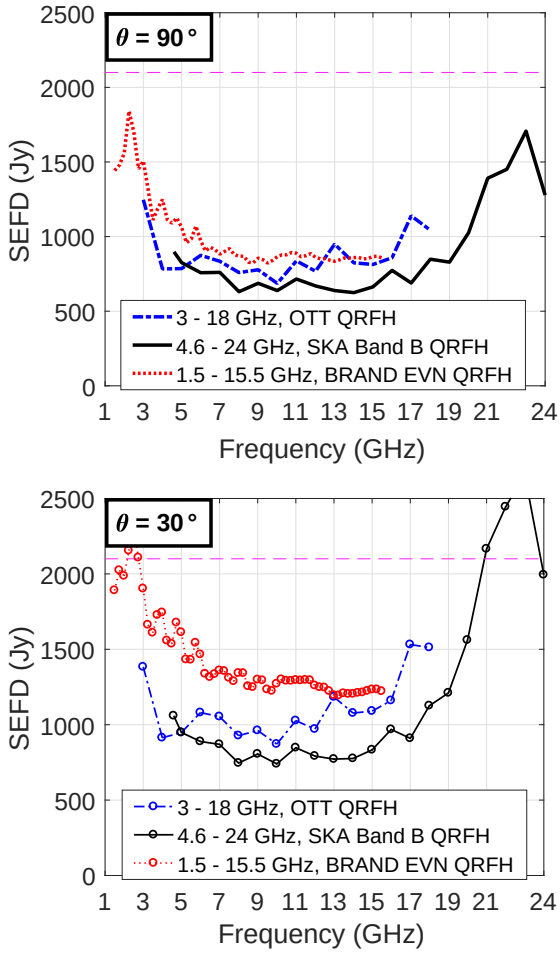

Fig. 3 Simulated SEFD over frequency at elevations $\theta = 90°$ (top) and $\theta = 30°$ (bottom) for the three receiver systems in the OTT reflector. Purple dashed line: 2,100 Jy.

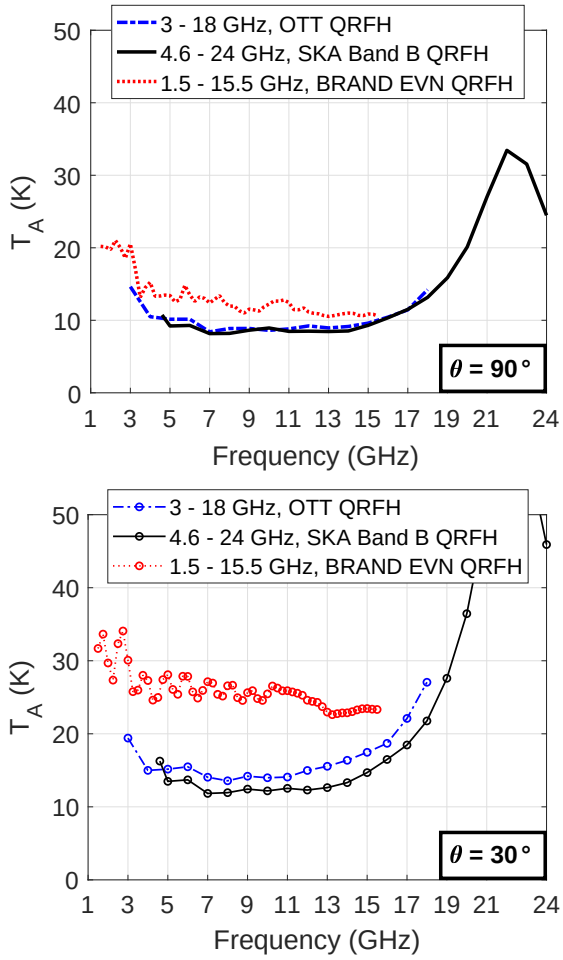

Fig. 4 Simulated T_A over frequency at elevations $\theta = 90°$ (top) and $\theta = 30°$ (bottom) for the three receiver systems in the OTT reflector.

slope of the spectra is affected by the absorption of liquid cloud water. The brightness temperatures in the $20-25$ GHz range are most sensitive to IWV, while frequencies above 30 GHz are most sensitive to ICW (where the general slope is not affected by the 22 GHz line), but frequencies below 20 GHz are also quite sensitive to ICW. IWV and ICW were estimated by polynomial expressions using the sky brightness temperatures (T_{b1} and T_{b2}) at two different frequencies (f1 and f2) for a given elevation. For IWV a second order polynomial was used:

$$IWV = a_0 + a_1 T_{b1} + a_2 T_{b2} + a_3 T_{b1}^2 + a_4 T_{b2}^2 + a_5 T_{b1} T_{b2} \quad (1)$$

For ICW a higher order polynomial was needed to generate a good fit:

$$ICW = b_0 + b_1 T_{b1} + b_2 T_{b2} + b_3 T_{b1}^2 + b_4 T_{b2}^2 + b_5 T_{b1} T_{b2} + b_6 T_{b1}^3 + b_7 T_{b2}^3 \quad (2)$$

The coefficients a_{1-5} and b_{1-7} were calculated using the method of least squares. Noise (σ_{T_b}) was added to the sky brightness temperatures, to simulate atmospheric variations and calibration noise. The polynomials in (1) and (2) were used to get the retrieved values of IWV and ICW. Finally the standard deviations between perfect fit and retrieved values were calculated.

Two-channel water-vapor radiometers were used for decades to estimate zenith wet delay as well as IWV and ICW. WVRs often use a frequency pair where the first channel is close to 21 or 24 GHz and the second is close to 31 GHz. In our study we first used f1 = 21 GHz and calculated the standard deviations when f2 varied between 15 and 35 GHz. As expected the frequency pair 21 and 31 GHz gave small retrieval errors, but the frequency pair 21 and 17 GHz also gave quite small retrieval errors. In the next step, f1 was set to 17 GHz, f2 varied between 15 and 35 GHz, and the calculations were done for different levels of atmospheric noise. It was then found that the frequency pair 17 and 23.4 GHz was a good choice, see Figure 5 (bottom). Finally the obtained results for the frequency pair 17/23.4 GHz were compared to 21/31 GHz. This comparison indicates that it is possible to use a frequency pair within the frequency range of the 4.6 – 24 GHz QRFH to obtain IWV and ICW to almost the same accuracy compared to a typical WVR, see Figure 6 (σ_{T_b} : 0.4 K). It is, however, important to note that this comparison is only valid if the calibrations of the 21/31 GHz and 17/23.4 GHz systems are performed to the same level of accuracy. Preliminary data indicate that the sky brightness temperatures at 17 and 23.4 GHz also can be used to estimate the slant wet delay, which can be very useful for VLBI observations. This will be discussed in an upcoming paper.

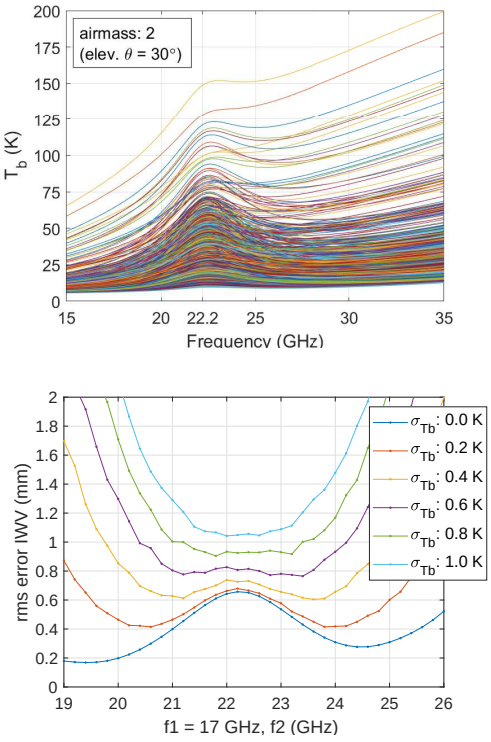

Fig. 5 (Top) Brightness temperature, T_b, of the sky at the Onsala site varying with ICW and IWV content; (bottom) RMS error in IWV varying with the choice of upper frequency channel, f2, and assumed σ_{T_b} rms noise error.

4 Conclusions

Simulations of the wideband systems developed for SKA and BRAND show SEFD performance similar to the current OTT system. The high-frequency limit of the 4.6 – 24 GHz QRFH presents an interesting application with telescope line-of-sight water-vapor radiometry during standard VLBI observations. This system will be set up and tested in the near future. RFI could potentially pollute the lower frequencies of VGOS, so the high cut-off frequency offered here may be beneficial in future systems.

Acknowledgements

The authors thank the ÅForsk Foundation for funding a travel grant for Jonas Flygare to attend the IVS 2018 conference and present this work.

References

1. J. Flygare et al., “Sensitivity and antenna noise temperature analysis of the feed system for the Onsala twin telescopes” in *Proc. 23rd EVGA Working Meeting (EVGA2017)*, Gothenburg, Sweden, May 2017.
2. B. Dong et al., “Optimization and Realization of Quadruple-ridge Flared Horn with New Spline-defined Profiles as a High-efficiency Feed for Reflectors over 4.6-24 GHz”, *IEEE Trans. Antennas. Propag.*, August 2017 (accepted for publ.).
3. J. Flygare, M. Pantaleev, and S. Olvhammar, “BRAND: Ultra-Wideband Feed Development for the European VLBI Network - A Dielectrically Loaded Decade Bandwidth

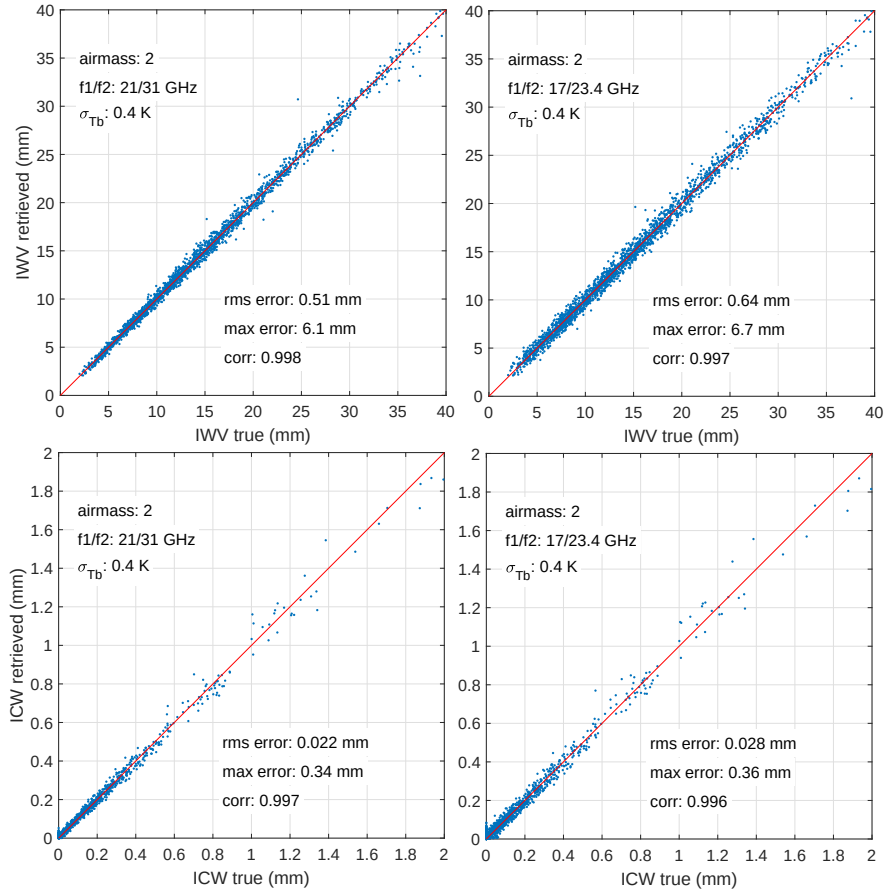

Fig. 6 (Top) IWV; (bottom) ICW; (left) simulated retrieved vs. true for the 21/31 GHz dedicated radiometer frequency channels; (right) simulated retrieved vs. true for the wideband feed 17/23.4 GHz frequency channels. $\sigma_{T_b} = 0.4$ K, $\theta = 30°$.

Quad-Ridge Flared Horn" in *Proc. 12th Euro. Conf. Antennas Propag. (EuCAP2018)*, London, UK, April 2018.

4. M. V. Ivashina et al., "An optimal beamforming strategy for wide-field surveys with phased-array-fed reflector antennas" in *IEEE Trans. Antennas Propag.,* vol. 59, no. 6, pp. 1864-1875, 2011.
5. B. J. Butler, "22 GHz Water Vapor Radiometry at the VLA", in *Imaging at Radio through Submillimeter Wavelengths, ASP Conf. Proc.*, Vol. 217, *ASP*, ISBN 1-58381-049-8, 2000., p.338, 2000.
6. P. Eriksson and G. Elgered, "Development of miniaturized microwave ground radiometers for satcom ground stations: Retrieval approach", *unpublished report*, patrick.eriksson@chalmers.se, 2016.
7. D. P. Dee et al., "The ERA-Interim reanalysis: configuration and performance of the data assimilation system", *Q.J.R. Meteorol. Soc.*, 137: 553-597, 2011.
8. S. A. Buehler et al., "ARTS, the Atmospheric Radiative Transfer Simulator", *J. Quant. Spectrosc. Radiat. Transfer*, 91:65-93, 2005.
9. P. Eriksson et al., "ARTS, the atmospheric radiative transfer simulator", version 2. *J. Quant. Spectrosc. Radiat.* Transfer, 112:1551-1558, 2011.
10. P. W. Rosenkranz., "Water vapor microwave continuum absorption: A comparison of measurements and models." *Radio Sci.*, 33(4):919-928, 1998 (correction in 34, 1025, 1999).
11. P. W. Rosenkranz., "Absorption of microwaves by atmospheric gases." In *Atmospheric remote sens. microw. radiometry*, pages 37-90. John Wiley & Sons, 1993.
12. M. Bevis et al., "GPS meteorology: Mapping zenith wet delays onto precipitable water", *J. Appl. Meteorol.*, 33:379-386, 1994.
13. H. J. Liebe, G. A. Hufford, and M. G. Cotton, "Propagation modeling of moist air and suspended water/ice particles at frequencies below 1000 GHz". In *AGARD 52nd Specialists Meeting of the Electromagn. Wave Propag. Panel*, Palma de Mallorca, Spain, May 1993.